Circulation and Dynamics of the Western North Atlantic. Part III: Forecasting the Meanders and Rings

A. GANGOPADHYAY* AND A. R. ROBINSON

Division of Applied Sciences, Department of Earth and Planetary Sciences, Harvard University, Cambridge, Massachusetts

(Manuscript received 26 April 1995, in final form 12 January 1996)

ABSTRACT

The multiscale feature models (MSFMs) developed for the circulation of the western North Atlantic (Part I) have been used for initialization in this study to forecast the Gulf Stream meanders and rings. The Harvard primitive equation model, which was calibrated and verified for the statistics of the synoptical dynamics in this region (Part II), provides the basis for these simulations. Three 2-week-long synoptical dynamical hindcasts are presented. These hindcasts are carried out in a forecast mode without assimilating any future information. In general, when compared against SST-derived frontal location and ring–stream interactions, 2-week-long forecasts are found to be statistically superior than persistence and dynamically consistent. These forecasts are also compared against similar forecasts based on the U.S. Navy's Optimum Thermal Interpolation System (OTIS) initializations. It is found that the MSFM-initialized simulations provide a better predictive capability than OTIS-initialized simulations over 2 weeks. Quantitatively, in terms of a statistical measure called the average offset of the axis of the stream, the former did better than persistence in all three cases over the 2-week periods. However, OTIS has two inherent characteristics, namely, a longitudinal distribution of temperature–salinity from climatology, and a warm pool at the core of the stream, which should be incorporated in the MSFM scheme to further enhance its predictive capability. The usefulness of multiscale kinematic synthesis in the initialization of the calibrated primitive equation dynamical model for forecasting the region over a 2-week period brings a closure to this three-part study of circulation and dynamics of the western North Atlantic.

1. Introduction

This study focuses on our present-day capability of forecasting the Gulf Stream meander and ring (GSMR) region. Using the Harvard primitive equation (PE) model as the dynamical basis, we investigate three 2-week data-rich periods from a viewpoint of synoptic verification. The initialization fields are based on the kinematic synthesis of multiscale feature models (MSFMs) as described by Gangopadhyay et al. (1997). For comparison, the forecasts are redone with the U.S. Navy's Optimum Thermal Interpolation System (OTIS) (Lai et al. 1994) initializations for the same periods. The verification dataset comprises nowcasts developed either by using MSFMs or by OTIS, as the case may be. These are based on the Gulf Stream (GS) axis locations, cold and warm ring location as determined by satellite infrared imagery, Geosat altimetry, and air-deployed expendable bathythermographs (AXBTs).

It is our intention here to underline the advantages and disadvantages of the two initialization procedures, namely, the MSFM kinematic synthesis and the OTIS initializations on the basis of their forecast skill in the GSMR region. For the three 2-week periods, both the MSFM and OTIS fields are dynamically evolved via the same dynamical model; no data have been assimilated during this period. The resulting 2-week evolutions are intercompared, both subjectively and quantitatively. The advantages, disadvantages, and some recommendations are then put forward.

Since the early 1980s, ocean forecasting has been progressively maturing with more and more sophisticated techniques available in other fields and following the lead from the meteorologists. Physically meaningful initializations and data assimilation are two of the recent approaches taken by ocean modelers to improve the predictive ability. Physical initialization is routinely being performed by meteorologists for short-term weather forecasts and analysis; however, application of such methodology in ocean forecasting has been limited to regional modeling and to a few investigators such as Robinson et al. (1988, 1989), Robinson (1992), Clancy (1987), Clancy et al. (1990), and Thompson and Schmitz (1989). The Harvard group had started the methodology for initializing a dynamical model via simple feature models (Robinson et al. 1988). This technique has fi-

* Current affiliation: Department of Physics, University of Massachusetts—Dartmouth, North Dartmouth, Massachusetts.

Corresponding author address: Dr. Avijit Gangopadhyay, Center for Marine Science and Technology, University of Massachusetts—Dartmouth, 706 S. Rodney French Boulevard, New Bedford, MA 02744. E-mail: avijit@atlantic.cmast.umassd.edu

TABLE 1. Simulation results. Here, "w" symbolizes a worse than persistence performance.

Analysis cases	Hindcast period	Initialization scheme	Persistence offset (km)		Improvement over persistence (%)	
			Day 7	Day 14	Day 7	Day 14
Case 1	6–20 May 1987	OTIS	44	58	24	11
		NOSBS	46	64	10	w
		SBS	46	64	38	16
Case 2	7–21 July 1987	OTIS	44	44	w	w
		NOSBS	43	50	19	22, w
		SBS	44	52	17	37*, 27
Case 3	4–18 May 1988	OTIS	41	46	27	8
		NOSBS	45	58	22	31
		SBS	45	58	20	15

* This value was attained on day 11; see text.

nally evolved to encompass the background circulation of the region and presented as the MSFMs in Part I by Gangopadhyay et al. (1995, hereafter GRA).

The importance of obtaining a dynamically balanced initial state for forecasts is also emphasized by Hulbert (1986), Hulburt et al. (1990), and Fox et al. (1993). Following a similar line of reasoning, using robust assimilation techniques to meld climatological datasets with few synoptic observations, Clancy et al. (1990) had developed the U.S. Navy's OTIS for initialization, called global OTIS. Subsequently, during the Data Assimilation and Model Evaluation Experiments (DAMEE), improved versions of the global OTIS were made available to users. In this study, we used the product from the version of OTIS after DAMEE phase III was concluded (Lai et al. 1994). This version is also referred to as the regional OTIS, which used a feature-model-based approach along with statistical interpolation for melding climatology. A version of regional OTIS is described by Cummings and Ignazewski (1991), and the details of the datasets used in this study are described in Lai et al. (1994).

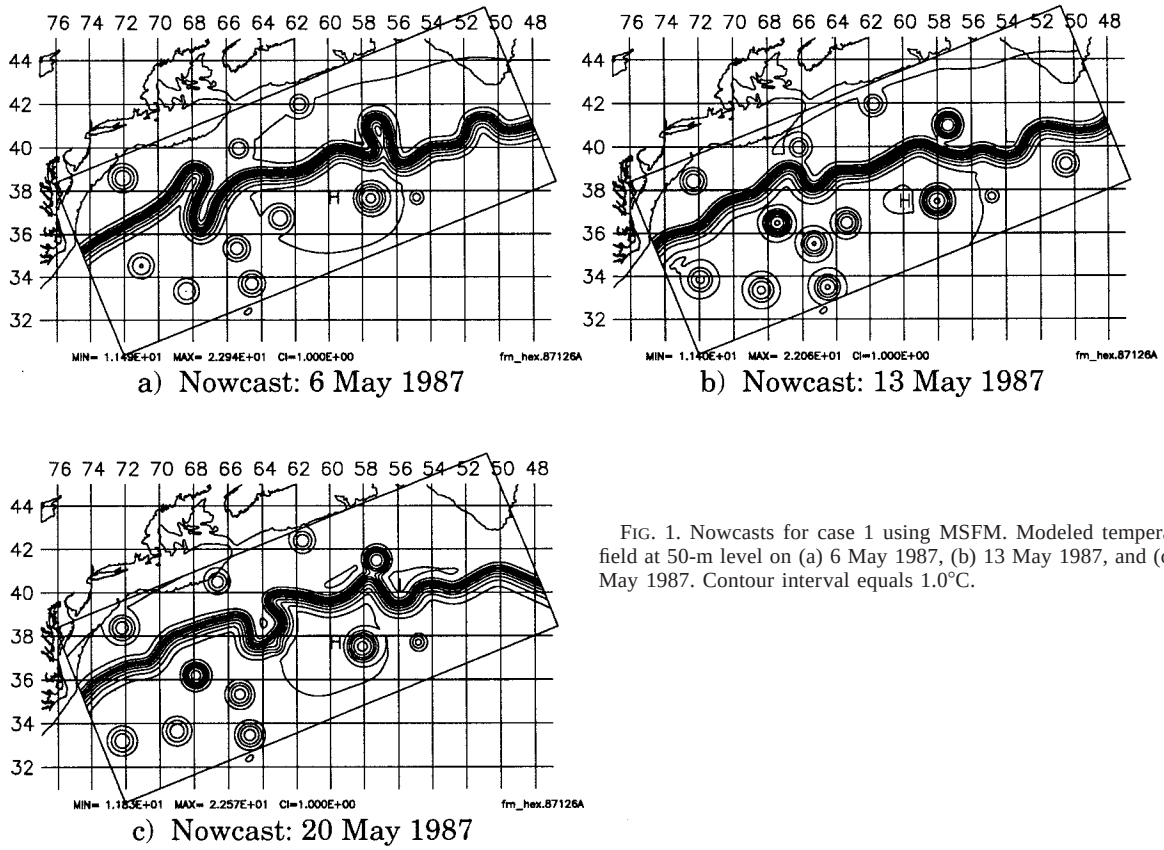

FIG. 1. Nowcasts for case 1 using MSFM. Modeled temperature field at 50-m level on (a) 6 May 1987, (b) 13 May 1987, and (c) 20 May 1987. Contour interval equals 1.0°C.

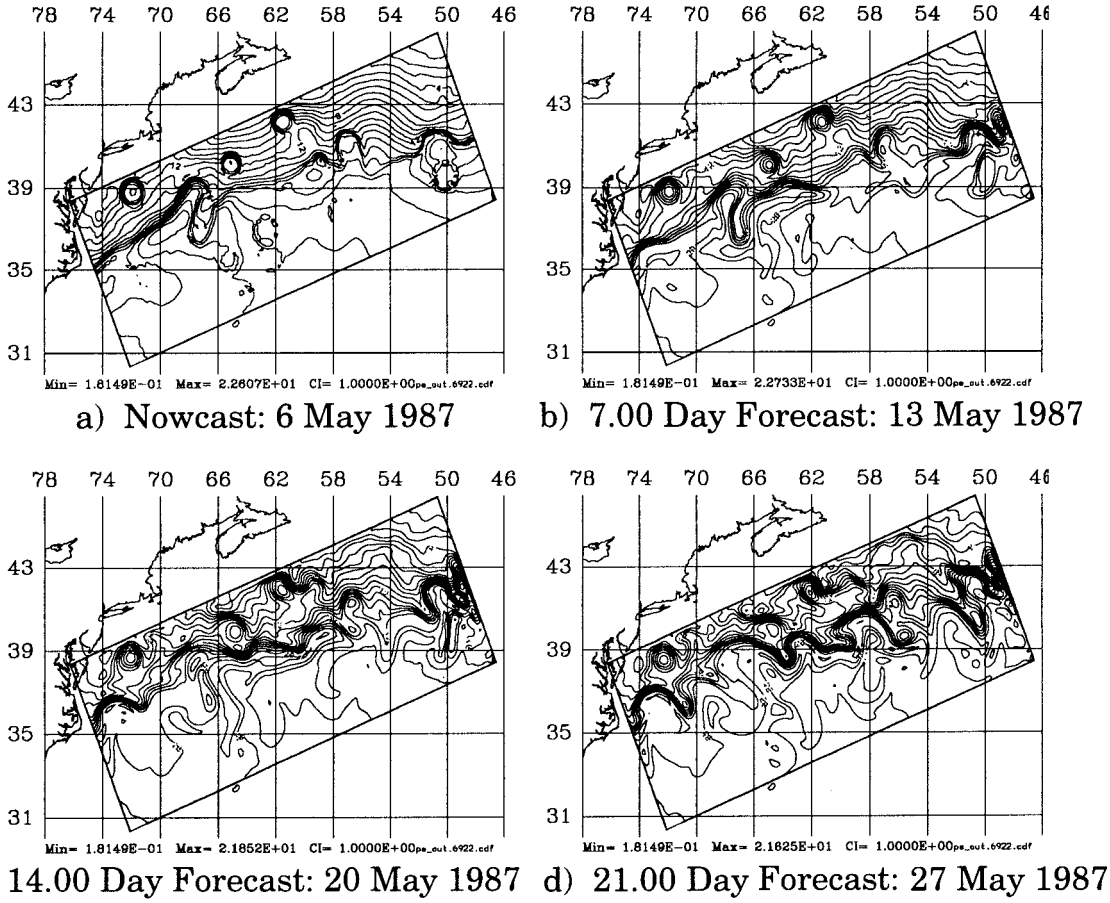

FIG. 2. OTIS nowcast and 3-week forecasts for case 1. Temperature fields at 50 m are shown for (a) initialization via OTIS for 6 May 1987, (b) 7-day forecast via primitive equation dynamics starting from (a), (c) day 14 of the simulation, and (d) day 21 of the simulation. Note how the Gulf Stream is becoming fragmanted later in the simulation. Contour interval equals 1.0°C.

It is important to understand our ability, or the lack thereof, in predicting the mesoscale variability of the real ocean. Mesoscale variability dominates major oceanic regions such as the western boundary currents like the GS, the Kuroshio, the Brazil current, the Somali current, etc. Predictive capability of such regions is linked to human utilizations of coastal resources as well as to our broader understanding of oceanic heat transport and large-scale short-term climate predictability. It is also equally important to generate four-dimensional data-driven simulations that are based on our current knowledge of the ocean, and to try to understand processes that would eventually lead to better numerical models. Current numerical models are often made to compromise on depicting certain processes via parameterizations (e.g., vertical mixing, lateral diffusion) due to constraints in resolution or computing power. Better understanding of such processes would eventually lead to adequate parameterization of turbulence. With these two goals in mind, we developed the advanced initialization methodology as described in detail by GRA.

Thus, it will be useful to investigate the impact of such initializations in forecasting the GSMR region. Clearly, a knowledgeable comparison of ocean forecasts via these two different initialization schemes would be very useful for future studies in oceanographic data assimilation and forecasting. We need to know how long the model realistically evolves in a mesoscale scenario before nonlinearity and other imperfections in our understanding of the ocean takes over the evolution. In atmospheric situations, we know that it is a matter of hours to days before the nonlinearities become important. The predictability of the ocean is largely dependent on the dynamics of each region; the equatorial ocean or noncoastal processes have different timescales than the Gulf Stream region studied here. In the GSMR region, we believe it is on the order of weeks. We shall see in this study that in three cases the MSFM does well for about 2 weeks, and that in one case it does well even for 3 weeks.

In recent years, several investigators from a number of institutions have embarked on a series of studies to realistically forecast the GS region. The DAMEEs have been carried out by scientists from MIT (Malanotte-M. Rizzoli and R. Young, manuscript submitted to *J. Atmos.*

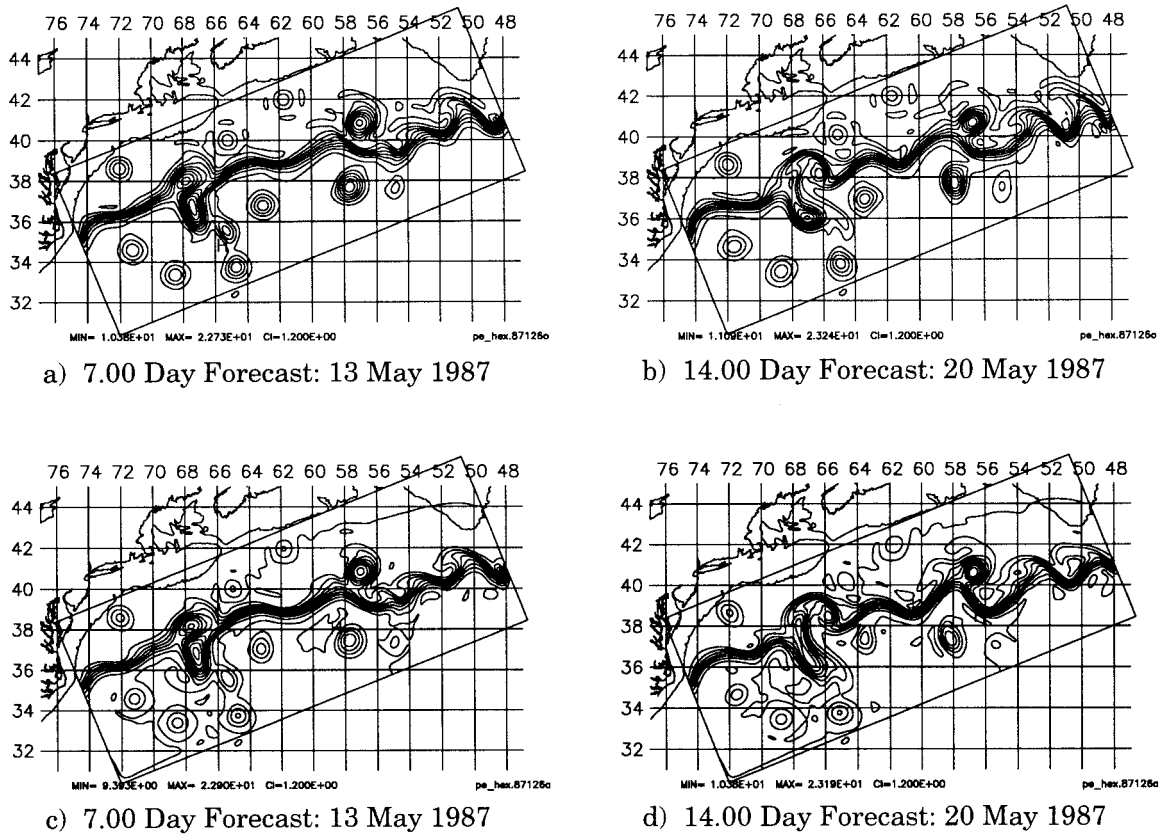

FIG. 3. MSFM-based 2-week forecast for case 1. Temperature evolution at 50 m are shown for (a) day 7 forecast starting from NOSBS initialization, (b) day 14 forecast from NOSBS initialization, (c) day 7 forecast from SBS initialization, and (d) day 14 forecast from SBS initialization. Contour interval equals 1.2°C.

Oceanic Technol.), Princeton (Mellor and Ezer 1991; Ezer et al. 1992; Ezer and Mellor 1994), and NRL-Stennis (Fox et al. 1992; Lai et al. 1994; Willems et al. 1994). The final conclusion of the DAMEE GSR study was that over a 2-week period, assimilating data (OTIS analyses) into the solution (hindcast) gave an improvement of 11%–37% when measured against persistence. This study (Willems et al. 1994) was for a 2-week period during 4–18 May 1988.

The GS meanders propagate and grow at a certain characteristic speed and rate; hence it is essential to reproduce such behavior in the dynamical model evolutions. The Harvard PE model has been calibrated and verified against such statistical measures as described in Part II by Robinson and Gangopadhyay (1997). In this part, we used the calibrated model as our basic dynamical platform for all the forecasts. This model is the open-ocean, hybrid-coordinate version of the Bryan and Cox (1967) PE model as described by Spall and Robinson (1989, 1990).

The organization of this paper is as follows. We discuss the datasets and the methodology of forecasting in the next section. The forecasts for the three case studies are then described sequentially in section 3. These results are discussed in section 4, and section 5 summarizes and concludes with certain recommendations.

2. Datasets and methodology

Three case studies were selected for this study. They are case 1—6–20 May 1987, case 2—7–21 July 1987, and case 3—4–18 May 1988. Their choice were dictated by their inclusion in the earlier DAMEE GSR studies (Lai et al. 1994; Willems et al. 1994). They are also the same cases for which Glenn and Robinson (1994) validated the Harvard Gulf Stream forecasting model based on the quasigeostrophic dynamics over 1-week periods. The high quality of the datasets for these three cases are described in detail by Glenn and Robinson (1994). It is important to note that the uncertainty in the GS axis and ring locations as observed by the AVHRR (Advanced Very High Resolution Radiometer) imagery is about ± 15 km.

The MSFM initialization procedure was described in detail by GRA and spared here for the sake of brevity. The MSFMs synthesize regional historical data. The elements of the feature model (the GS; rings; recirculation gyres; and the deep western boundary current,

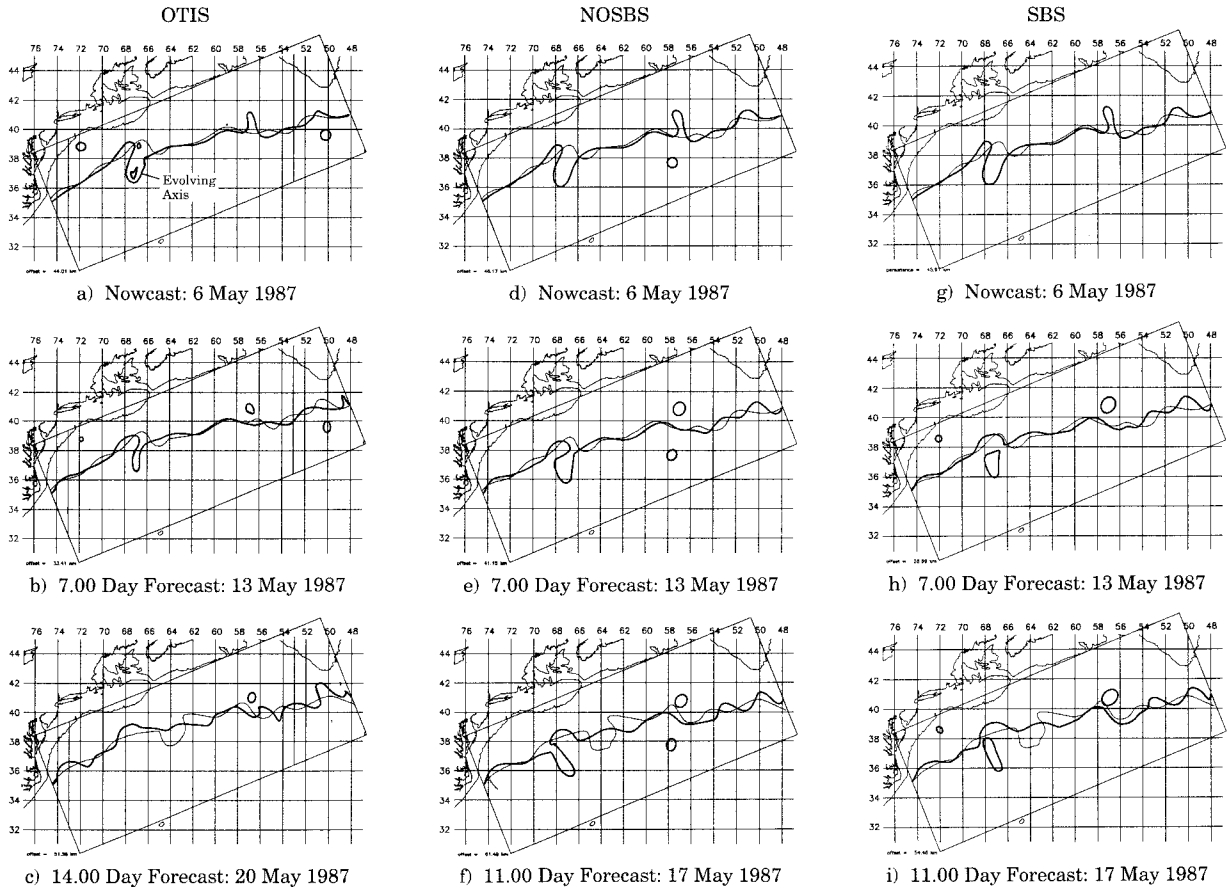

FIG. 4. Intercomparison of 15°C isotherm location at 150 m for the three simulations for case 1. (a) OTIS-derived day 0 and day 7 nowcast axis locations; (b) axis location on day 7 extracted from PE simulation (started from OTIS on day 0) against OTIS nowcast on day 7; (c) axis location on day 7 from PE via OTIS against OTIS nowcast on day 14 from data; (d), (e), and (f) are similar to (a), (b), and (c) except for NOSBS simulation; (g), (h), and (i) are similar to (a), (b), and (c) except for the SBS simulation. Note that the thick line in each panel is the axis extracted from the simulation (forecast) and the thin lines are the nowcast.

called DWBC) have been linked together via mass conservation, and the range of the parameters of the feature models are determined by the statistics of the variability of the regional hydrographic and velocity data (GRA). Using such methodology, initial three-dimensional fields of temperature, salinity, and velocity are generated from minimal observations available from ship, bathythermographs, buoy deployments, and satellite IR imagery. The initializations available from regional OTIS used only a front and eddy bogus (and time of year) for its feature model approach, satellite-derived MCSST fields, XBT, ship's observations, buoys, and GDEM climatology. The detail statistical interpolation technique using point observations and climatology background is summarized by Lai et al. (1994). Note that while both initializations uses similar input observations and generates similar fields (*T, S, U, V*) for the prognostic PE model, the MSFM methodology uses kinematic synthesis of the different elements of the regional circulation in a velocity-based feature model approach where the initial mass and velocity fields are dynamically adjusted, whereas the OTIS methodology melds climatological temperature–salinity (*T–S*) to sparse observations via statistical interpolation and derives the velocity fields from inferred two-dimensional dynamic height fields.

Once the initializations are obtained, they are evolved by the Harvard open ocean PE model for 2–4 weeks as the case may be. Table 1 shows the different model runs carried out for each of the three synoptic cases. Three different initializations were used in each case study. The first one is the U.S. Navy's OTIS initialization (these fields were kindly provided by A. Lai). The other two are based on the MSFM scheme. The difference between the second and the third type of initialization is that the second model did not have the subbasin-scale (SBS) features enabled (called NOSBS), and the third model is the full scheme with the recirculations and the DWBC, with parameters tuned and calibrated for the summer transport as described in Part II of this study, called SBS. We refer to the second type of initialization as the NOSBS case, whereas the third one is rightfully referred as the SBS case. Note also that the stream in

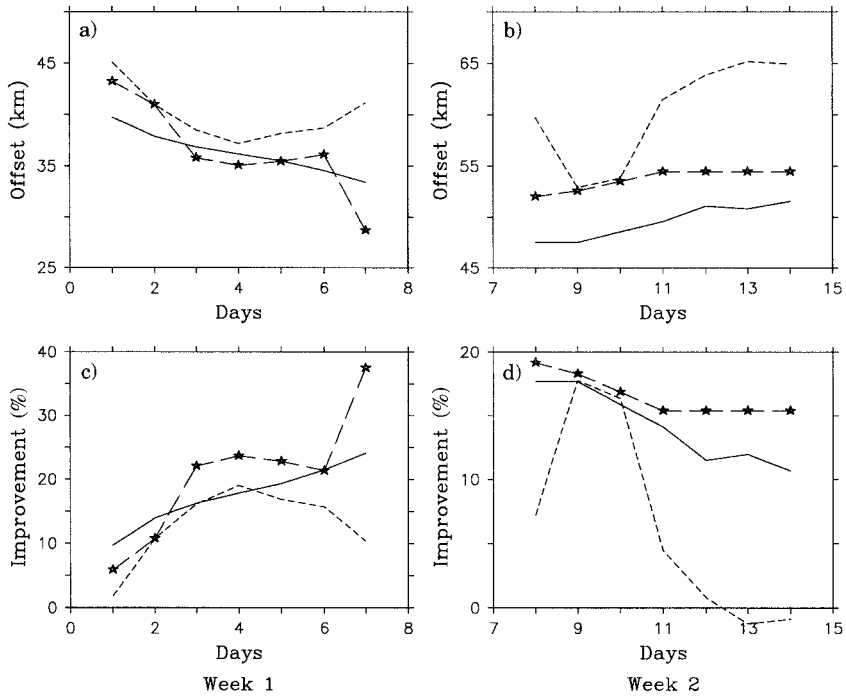

FIG. 5. Offset and improvement statistics for 2-week simulations during 6–20 May 1987. (a) Offset for week 1, (b) offset for week 2, (c) improvement over persistence over week 1, and (d) improvement over persistence for week 2. Solid line is for OTIS, dashed line is for NOSBS, and the star–dash line is for SBS. The improvement for week 1 is computed as $i_1 = (p_1 - d_i)/p_1 \times 100$, and for week 2 as $i_2 = p_2 - e_i/p_2 \times 100$. Here, p_1 is the average offset between the nowcasts on day 0 and day 7, whereas p_2 is the offset between the nowcasts on day 0 and day 14. Also, d_i is the offset between the forecast on day i and the nowcast on day 7, whereas e_i is the offset between the forecast on day i and nowcast on day 14. For this case, p_1 equals 46 km and p_2 equals 64 km for both the NOSBS and SBS simulations, and p_1 equals 44 km and p_2 equals 58 km for the OTIS simulation (see Table 1).

the NOSBS case carries a constant transport, similar to that used by Glenn and Robinson (1994), albeit improved by the synoptic profile developed in GRA.

The measure of performance was based on two criteria. The first measure was to subjectively compare the forecast temperature field from each day of the 2-week forecast with the nowcasts at day 7 and day 14. The subjective determination of success includes realistic meandering and occurrences of major events such as ring formations, absorptions, or mergers. The ability or limitation of different simulations to evolve realistically is described in detail for each case separately in the next section. The second measure was to compute the average offset between the forecast location of the 15°C isotherm at 150 m and that from the nowcasts. Note that the 15°C/150 m is chosen as the axis because 150 m is one of the model levels and it is closest to the more common 15°C/200 m definition of the axis. The reason for choosing 15°C/200 m as the axis of the GS had been validated by Cornillon and Watts (1987). This typical statistical measure has also been used by Glenn and Robinson (1994) and by Willems et al. (1994). The average offset calculation was made between 73° and 53°W because this area had full data coverage, and this area is also distant enough from the boundaries to remain unaffected by persisted boundary conditions imposed in the dynamical runs.

3. Hindcast simulations

The three simulations and their results are presented in Table 1 and described in this section. For the sake of brevity, each case study is illustrated by a suitable set of figures. Each set starts with the initializations and weekly nowcasts over the study period, followed by the forecasts. MSFM-based forecasts are compared against MSFM-based nowcasts on days 7 and 14; OTIS-based forecasts are compared against OTIS-based nowcasts on similar days. Such intercomparison minimizes the effect of statistical interpolation or kinematic synthesis on the evaluation of forecast skill for the dynamical simulations. The comparative evolution of the GS axis (15°C isotherm at 150 m) for three different initializations for each case (except the last case) is then shown followed by the forecast skill measures. Note that the average offset of persistence, as depicted in Table 1 for day 7, is determined from the difference in axis locations extracted from the nowcasts on day 0 and day 7. Similarly,

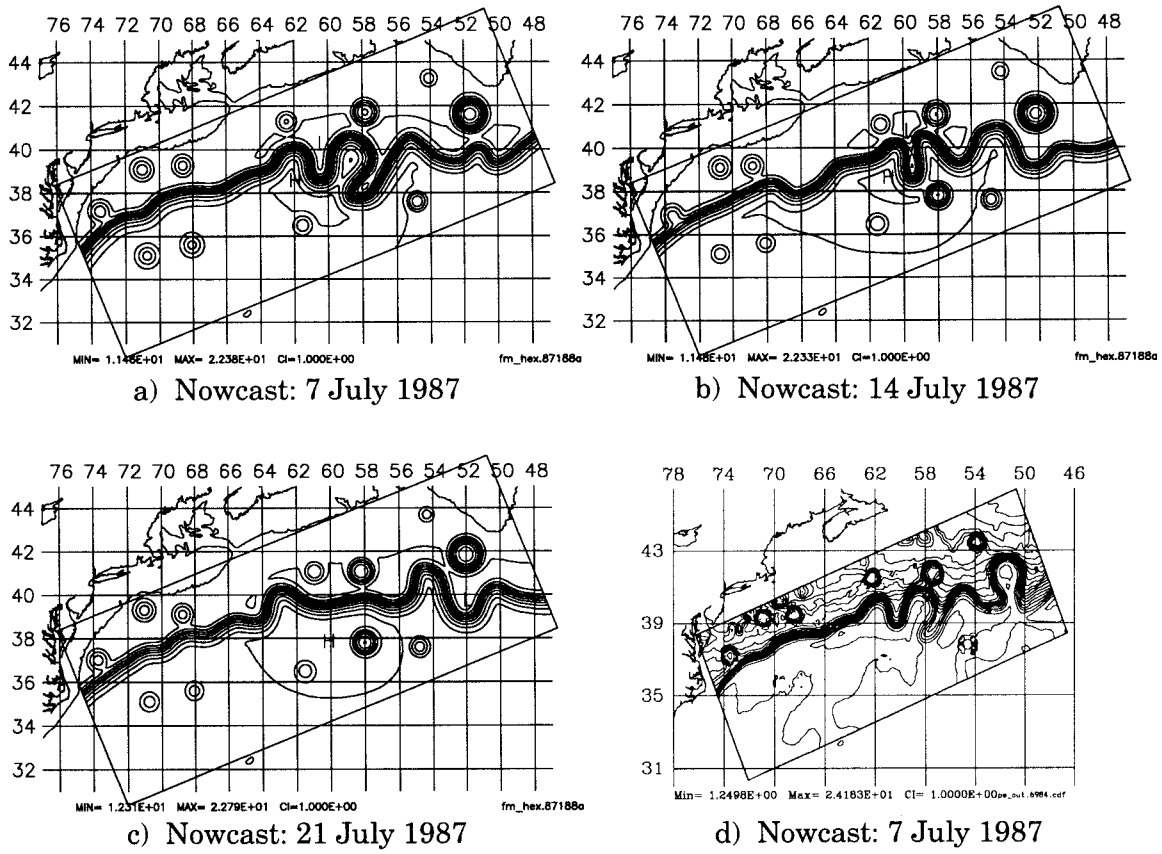

FIG. 6. Nowcasts for case 2 (7–21 July 1987). Modeled temperature fields at 50 m using MSFM are shown here for (a) 7 July 1987, (b) 14 July 1987, and (c) 21 July 1987. Temperature initialization at 50 m via the OTIS-derived nowcast on 7 July 1987 is shown in (d). Contour interval equals 1.0°C.

the persistence offset for day 14 is obtained from the difference between nowcasts on day 0 and day 14.

a. Case 1—May 1987 (87126)

The nowcast fields on 6, 13, and 20 May 1987 are shown in Fig. 1. These are based on NOAA IR, Geosat, AXBT datasets and are kinematically synthesized by the initialization methodology described by GRA. There are three warm core rings (WCRs) and seven cold core rings (CCRs) on 6 May, the starting day for the 2-week forecast. The GS is seen to be meandering northeastward with a Z-shaped meander in the 70°–66°W region, and with a warm ring about to be born at 57°W. There are three events that occur in nature during the first week. These are 1) a CCR forms by day 7 at 67°W, 2) the crest at 68°W interacts with the adjacent WCR at 66°W and helps form a trough at 65°W, and 3) the WCR at 57°W is fully formed. During the second week the stream maintains most of its earlier configuration, except that the trough at 65°W interacts with the CCR at 64°W and forms a rather broad trough centered at 64°W.

Figure 2 shows the OTIS initialization and the forecast fields for days 7, 14, and 21. As seen in all OTIS nowcasts, the slope water side is heavily crowded with strong temperature gradients. The minimum temperature at the surface for OTIS fields often approaches 0°C. As seen in the forecast fields, this simulation does not give birth to the two rings during the first week. As will be explained later, the predicted path of the Gulf Stream is also not significantly different from the persistence measure. As is clear from Fig. 2, the Gulf Stream becomes a joining of filaments, losing its integrity over the domain during the second and third week of simulation. Also note the formation of strong jets and filaments on the slope water side unlike the real ocean, which is a result of the presence of a rather unnatural temperature gradient in the initialization.

The corresponding 2-week simulations using the MSFMs are shown in Fig. 3. The forecasts on day 7 and day 14 for the NOSBS case are shown in Figs. 3a and 3b, whereas those for the SBS case are presented in Figs. 3c and 3d, respectively. It is evident that during the first week the CCR formation at 67°W is realized by both the NOSBS and the SBS simulations. The OTIS evolution could not simulate this event in the first week. The ring detachment happens in the NOSBS case later in the simulation during the second week. The WCR

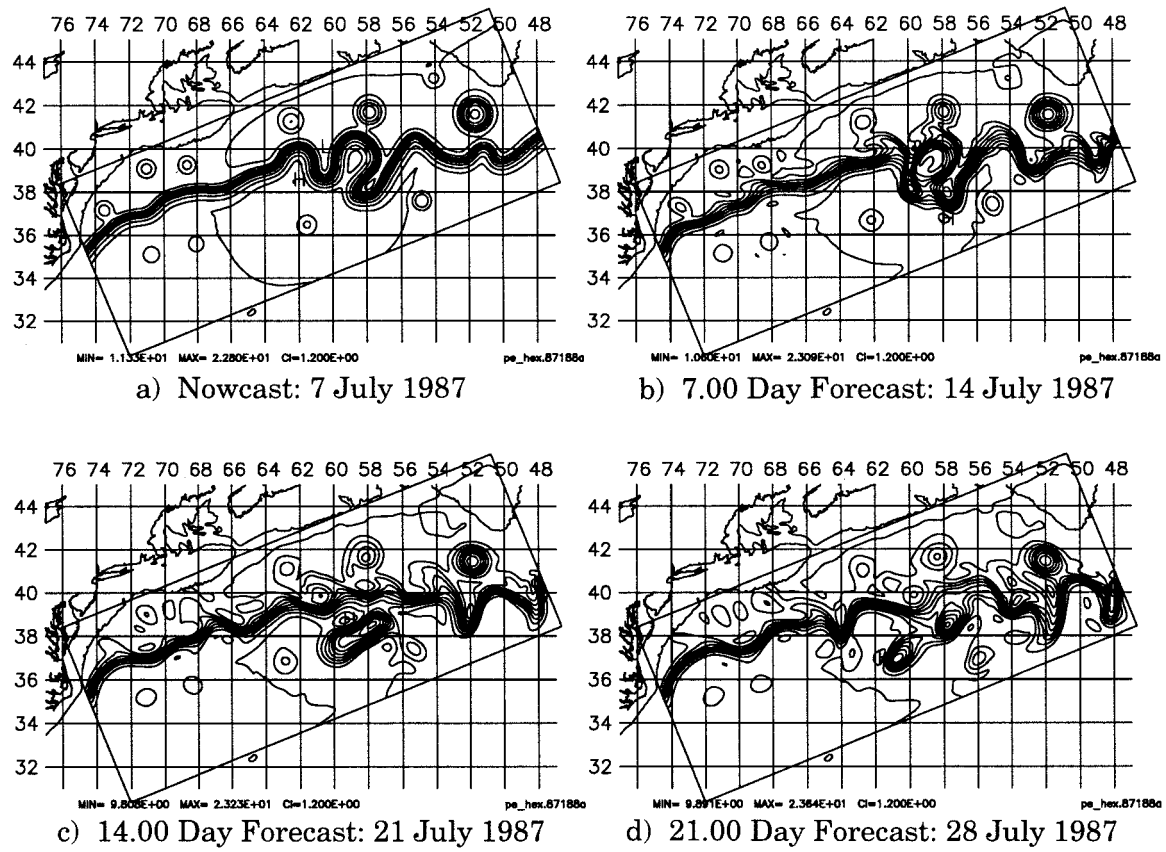

FIG. 7. SBS nowcast and 3-week forecast for case 2. Temperature field at 50-m level are shown for (a) initialization, (b) day 7 forecast, (c) day 14 forecast, and (d) day 21 of the forecast. Contour interval equals 1.2°C.

formation at 57°W is again predicted by both NOSBS and SBS simulations during the first week. It is interesting to note that the propagation of the crest from 68° to 66°W during the 2-week simulation is realistically evolved only by the SBS simulation. This is due to the inclusion of SBS features in the initialization and proper calibration of the wave-growth characteristics for the MSFM-based scheme as described in Robinson and Gangopadhyay (1997, hereafter referred to as RG).

The next three panels in Fig. 4 present the comparison of the extracted 15°C isotherm at 150 m for the 2-week evolution against that from the nowcasts for each of the three different simulations for this case. Note the inability of the OTIS and NOSBS simulations to detach the CCR at 67°W (Figs. 4b and 4e), however, the SBS simulation detaches a large cold core blob by day 7. Note also that the 14-day evolution for the OTIS has finally detached that blob, although the meander growth is out of phase with the nowcast during most of the area between 73° and 53°W. The MSFM simulations are shown only on day 11 for the second week since the blob formed by day 7 in the SBS simulation reattaches to the stream on day 12. The NOSBS simulation fails to detach this blob during this week. It is interesting to note that the SBS simulation has developed meanders very much in phase with the nowcasts between 73° and 53°W over these 2 weeks.

Figure 5 depicts these results quantitatively in four panels. The top panels show the offset measures as a function of days. The offset is defined by the ratio of the area between the forecast and the nowcast stream axes to the average axis length between 73° and 55°W. For week 1, persistence offset is the offset between nowcasts on day 0 and day 7. For week 2, persistence offset is computed from the nowcasts on day 0 and day 14. The forecast offset during any day of week 1 is determined from the forecast on that day and the nowcast on day 7. Thus, if the evolution is realistic during the first week, the forecast offset will be minimum on day 7 decreasing from the maximum for the persistence offset on day 0. As mentioned before, OTIS forecasts are compared against OTIS nowcasts at a later day, and MSFM-based forecasts are evaluated against MSFM-based nowcasts on later days.

The bottom panels in Fig. 5 show the improvement of prediction over persistence as a function of days. The exact mathematical expression for obtaining the percent improvement is given in the caption for this figure. The left panels are for the first week of the simulation and the right panels are for the following week. Each panel

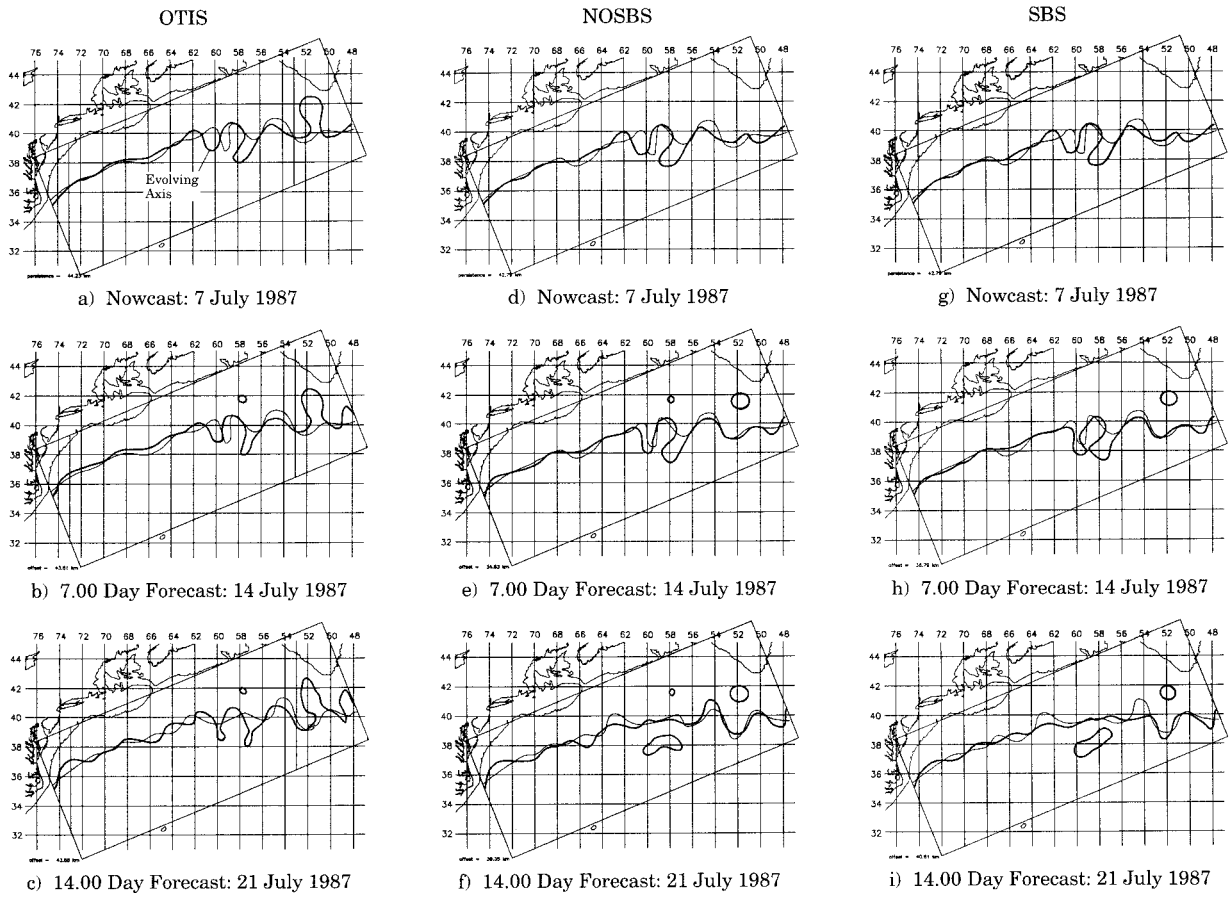

FIG. 8. Intercomparison of 15°C isotherm location at 150 m for the three simulations for case 2. (a) OTIS-derived day 0 and day 7 nowcast axis locations; (b) axis location on day 7 extracted from PE simulation (started from OTIS on day 0 against OTIS nowcast on day 7); (c) axis location on day 7 from PE via OTIS against OTIS nowcast on day 14 from data. Panels (d), (e), and (f) are similar to (a), (b), and (c) except for NOSBS simulation. Panels (g), (h), and (i) are similar to (a), (b), and (c) except for the SBS simulation. As in Fig. 4, the thick lines are forecast axes, and the thin lines represents the respective nowcast axes.

shows the results for three simulation cases—the solid line is for the OTIS, the dash line is the NOSBS case, and the star-marked solid line is for the SBS simulation. It is generally observed that the OTIS fields have the minimum persistence offset; we believe this is a result of optimum interpolation of available datasets in the initialization stage. However, the decrease in offset during the first week of simulation is not statistically significant for the OTIS case; that is, the improvement over persistence is within the error bounds (±15 km) of the initialization–verification dataset. As is shown in this figure, the SBS simulations are the best for most of 2-week period, the maximum improvement of 38% is achieved on day 7. The SBS prediction for the second week is statistically significant at the 75% confidence level in that the improvement of 15%–20% over persistence of 52 km is 75% better than the verification error of 25 km.

b. Case 2—July 1987 (87188)

The MSFM-derived nowcasts for this case for days 0, 7, and 14 are shown in Figs. 6a–c. For the most part of the domain the stream maintains its meandering path during the 2-week period. The major events are centered near 62°–56°W region. In the MSFM initialization, there are seven WCRs and four CCRs. However, in the OTIS initialization there are only six WCRs. The CCR at 52°W is treated as part of the stream (see Fig. 6d), which leads to unrealistic long filaments near the eastern boundary of the domain after the first week of dynamical evolution. Similar to case 1, this OTIS initialization also suffers from an abundance of isotherms in the slope water side.

The MSFM initialized primitive equation model simulations for the 3-week period are shown in Fig. 7 for the SBS case. The comparative evolution of the 15°C isotherm for all three cases is shown in Fig. 8. It is interesting that during the first week, OTIS, NOSBS, and SBS could not evolve into a ring birth at 58°W. However, the SBS simulation is very close to detaching a ring at 60°W. During the second week, contrary to nature, OTIS simulation predicted interaction of the stream with both the rings; however, one could argue

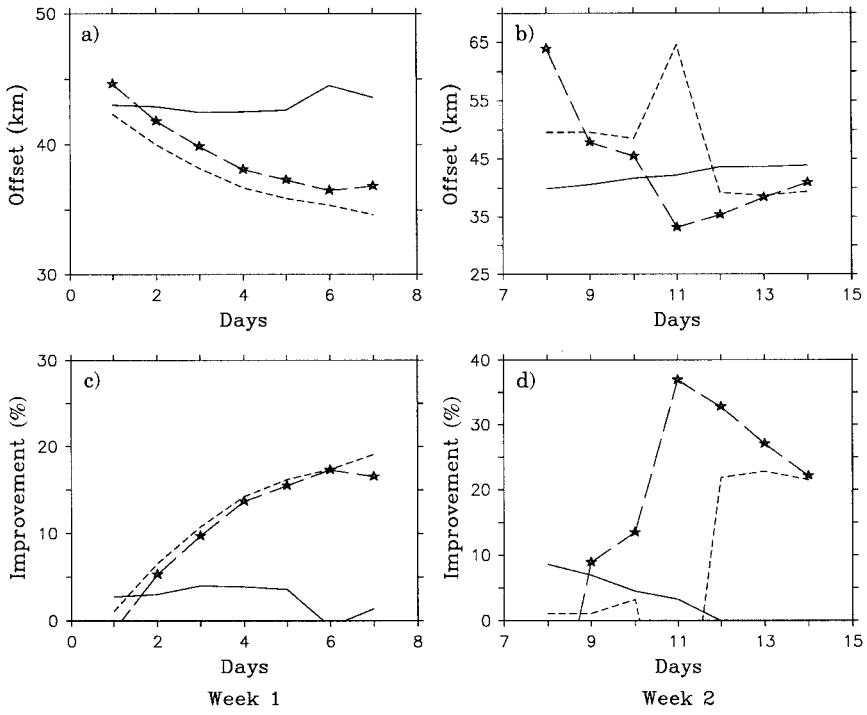

FIG. 9. Offset and improvement statistics for 2-week simulations in case 2. (a) Offset for week 1, (b) offset for week 2, (c) improvement against persistence over week 1, and (d) improvement against persistence over week 2. The solid line is for OTIS, the dashed line is for NOSBS, and the star–dash line is for the SBS simulations. Please see caption of Fig. 5 for a detailed explanation of how the statistics are obtained.

that the ring at 58°W is born already and the one at 60°W will be born in a day or two. For the NOSBS simulation, during the second week, a large bicentric blob is formed in the 60°–58°W region, which becomes a large blob of cold core by day 21. The SBS simulation behaves similarly to the NOSBS simulation for the first 2 weeks; however, interestingly, the bicentric blob in this case clearly separates out into two distinct rings by week 3 (see Fig. 7d). The IR analyst could identify these two separate rings on the 28 July 1987 imagery.

The tendency of OTIS evolutions to go out of phase with OTIS nowcasts is evident in Figs. 8a–c. The NOSBS and SBS cases have little differences in the first week of simulation; however, they differ qualitatively as well as quantitatively during the second week. It is shown that SBS is consistently doing better than NOSBS for longer-term simulations because of its inclusion of SBS recirculation gyres and the transport variation mechanism built in for the Gulf Stream. Note that the stream in the NOSBS case is, on the other hand, a constant transport stream, much like the ones used by Glenn and Robinson (1994).

The statistical results are presented in Fig. 9 in a similar fashion as for case 1 in Fig. 5. In this case, both the NOSBS and SBS simulations tracked the stream path well enough to result into a statistically significant prediction, which is better than persistence. For the OTIS case the offset stays almost the same for most of the period; however, it increases on days 6 and 7. The NOSBS case does marginally better than the SBS case for the first 5 days. During the second week, SBS does consistently better than both OTIS and NOSBS simulations. The maximum improvement of 37% for the SBS case is achieved on day 11 when the two-ring blob detaches from the stream. On day 14, the improvement over the region 73°–53°W for the SBS simulation is 22% better than persistence.

c. Case 3—May 1988 (88125)

The nowcasts for this case are shown for 3 weeks starting on 4 May 1988 in Fig. 10. This particular case has been presented by Willems et al. (1994) in detail based on an OTIS initialization. There are six WCRs and six CCRs in the initialization on 4 May 1988. The stream is smoothly meandering throughout the domain with a crest–trough combination in the 66°–60°W region. During the first week, one WCR formed at 65°W, and the following trough tightens around itself at 62°W. During the second week, this trough almost detaches from the stream and forms a looping meander whose crest at 62°W interacts with a small WCR between 62° and 63°W. In the third week, the CCR formation is complete, and the crest–ring interaction results in a large-amplitude meandering crest centered at 62°W.

In this case, the dynamical evolution of the OTIS

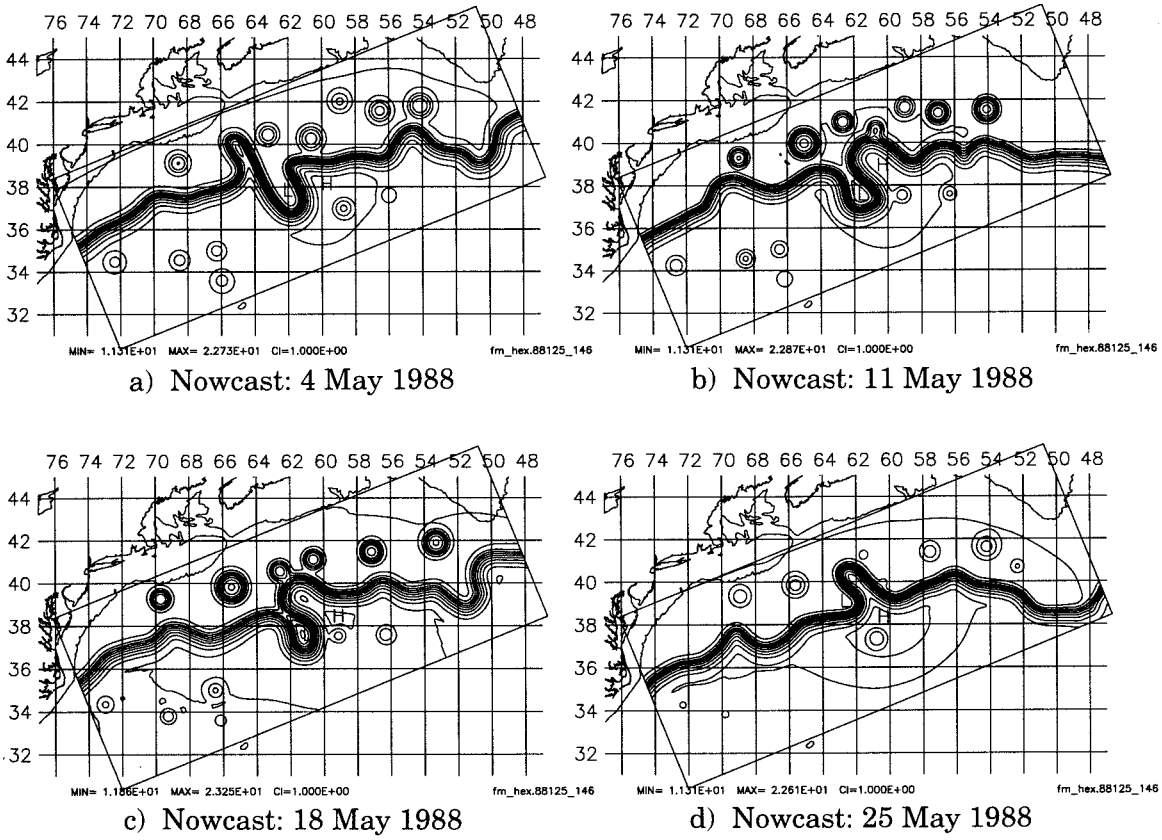

FIG. 10. Nowcasts for case 3 using SBS-based MSFM. Temperature fields at 50-m model level are shown for (a) 4 May 1988, (b) 11 May 1988, (c) 18 May 1988, and (d) 25 May 1988. Contour interval equals 1.0°C.

fields is again noticeably noisy with the Gulf Stream breaking into large interacting filaments during the second week and becoming unrealistic by the middle of the third week. However, this particular OTIS initialization has a very realistic warm core Gulf Stream and performs the best dynamically among the three cases during the first week. This is not shown here, although the interested reader may look into Willems et al. (1994).

The MSFM initialized forecasts (SBS only) are presented in Fig. 11. Both the SBS and NOSBS cases have successfully formed the WCR at 65°W during the first week. The tightening of the trough at 62°W is more pronounced in the SBS case than in the NOSBS case. During the second week, this tightening continues and finally in the third week the SBS case realistically detaches the CCR at 62°W; whereas the NOSBS simulation still predicts a yet-to-be-born ring event. The stream meandering is also more continuous for the SBS case than in the NOSBS case for the third week. It is also important to note that when the SBS simulation is further carried out, the CCR formed at 61°W detaches from the stream on days 22–23 and moves in the south-southwestern direction at a background speed of 5 km day^{-1}.

In this case study, the OTIS simulation does better than both the NOSBS and SBS simulation in the statistical measure of offset during the first week (see Fig. 12). This is because the OTIS initialization fields in this case are well assimilated with information from the future evolutions, which reduces the offset between the initialization and the weekly nowcasts as well as reduces the offset during the evolution in the first week. However, during the second week, OTIS evolutions are marginally satisfactory (10% better than persistence). The NOSBS simulation performs significantly better than SBS in the second week (Figs. 12b and 12d) because of an interaction of the stream with the ring at 60°W (See Fig. 11d), which unfortunately does not happen in the SBS case.

Given the complicated nature of computing the statistics, and not to be biased by a single statistical measure, it is prudent to analyze the overall simulations from a pragmatic point of view. It is clear that the SBS simulation is more realistic for the stream, the rings, and the surrounding waters than depicted by either the NOSBS or the OTIS simulations. Also, the SBS simulations are the only ones that could be carried out realistically within the error bounds of the initialization–verification datasets for more than 2 weeks.

4. Discussion

The numerical simulations carried out in this study and described in the previous section bring out several

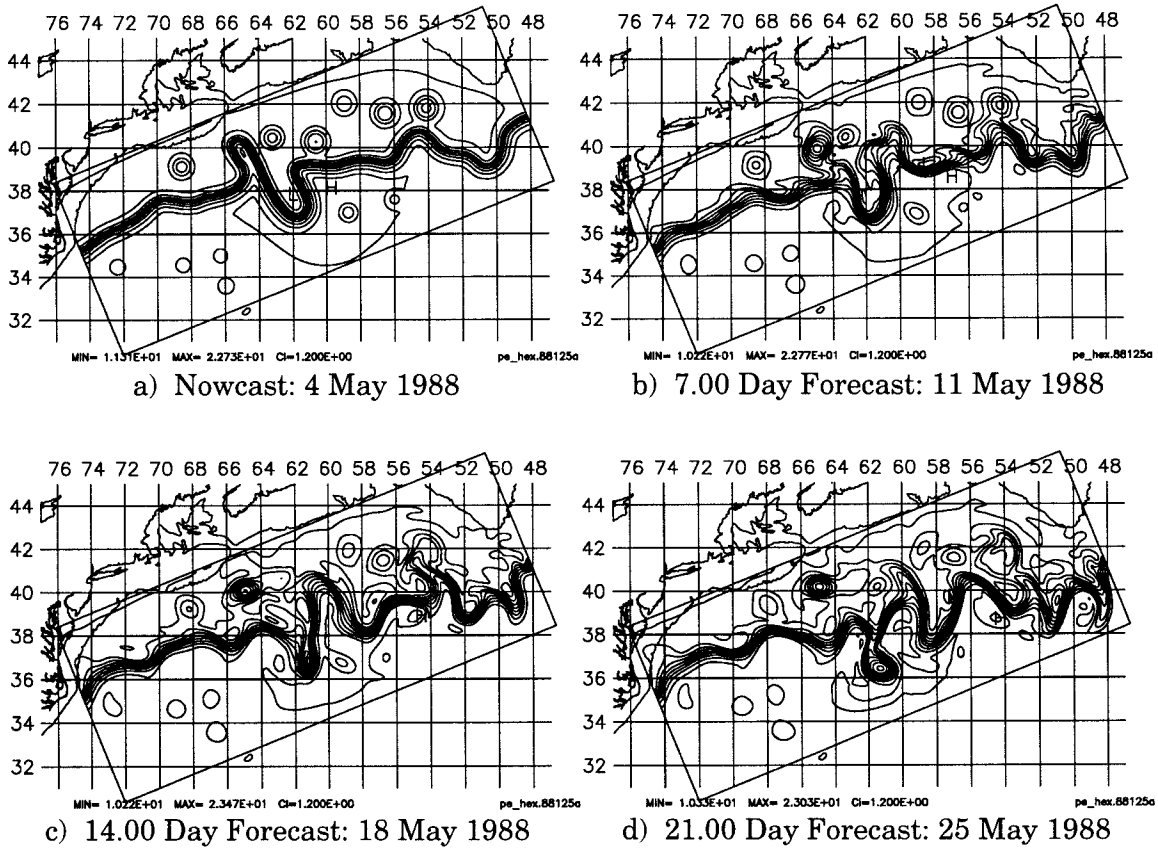

FIG. 11. SBS nowcast and 3-week forecasts for case 3. Temperature fields at 50-m model level are shown for (a) initialization, (b) day 7 forecast, (c) day 14 forecast, and (d) day 21 of the forecast. Contour interval equals 1.2°C.

insights into the mesoscale ocean forecasting capability in the Gulf Stream meander and ring region. It is clear that it is now possible to predict the location of the stream over a period of 2 weeks and that the predicted path would be better than using persistence over 2 weeks. It is also possible to reinitialize at the end of week 1 with new data during the first week to have a better forecast at the end of the second week. The reinitialization methodology is very common in weather forecasting and was adopted in the operational gulfcasting by Robinson et al. (1989) in a quasigeostrophic dynamical system, which had a reasonable forecast skill over a 1-week period (Glenn and Robinson 1994).

We have shown that the GS meandering and ring–stream interactions are well reproduced via a primitive equation model and a novel initialization methodology. The success of our system is achieved due to two important factors: 1) the concept of kinematic synthesis of all necessary elements of the regional circulation system in the initial state and 2) the parametric sensitivity analysis as described in RG to calibrate the dynamical model to the statistics of synoptical dynamics in this region. The first one is similar to the so-called physical initialization in meteorological forecasting.

The major difference between the two initializations (MSFM and OTIS) considered is the way the three-dimensional fields are brought together at the initial state. The OTIS fields are generated via optimal interpolation of available data with hydrographic climatology that naturally produces realistic temperature and salinity features but unassumingly create some unwanted features because of statistical interpolation. The high surface gradient of temperature north of the GS in this version of the regional OTIS is due to the absence of the polar front. Another drawback of the OTIS fields is the assumption of a level of no motion in the 1000-m range results in a rather weak surface velocity for the GS and that this prohibits any realistic representation of the real ocean below the main thermocline, such as the DWBC and abyssal parts of the recirculation gyres. In spite of such restrictions, it is interesting to note that the OTIS-initialized cases do quite well for a 1-week period. The major advantage of OTIS is its thermal structure, that is, the longitudinal variation of *T–S* properties along the axis of the stream (provided by climatology) and the presence of a warm pool of water along the axis of the GS in the top 200 m of water column. This pool is very realistic, and we believe this structure provides the stable performance of OTIS in predicting the GS path in the first week of the hindcasts

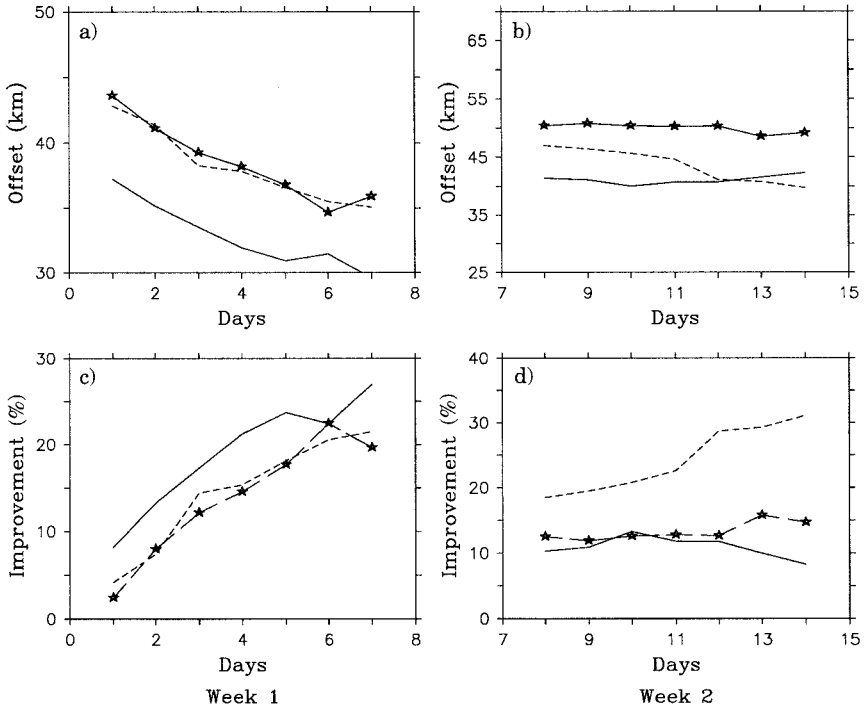

FIG. 12. Offset and improvement statistics for 2-week simulations in case 3. (a) Offset for week 1, (b) offset for week 2, (c) improvement against persistence over week 1, and (d) improvement against persistence over week 2. The solid line is for OTIS, the dashed line is for NOSBS, and the star–dash line is for the SBS simulations. Please refer to Fig. 5 caption and Table 1 for details of offset and improvement computational procedure.

before being taken over by the surrounding nonlinear growths and unwarranted interactions between the stream and similarly strong filaments in the surrounding waters. Another weakness in this particular version of OTIS fields was the lack of observed eddies in the initial state. This could be a matter of deception also, especially in the slope waters, where the relatively weaker thermal gradients might get mixed in the stronger unrealistic frontal gradients present in this version of OTIS.

The MSFM fields are, on the other hand, designed on the basis of the velocity fields of the pertinent features first, and then the *T–S* distribution is obtained via the water-mass analysis of the region (GRA). This approach is better suited for the active regions of the ocean such as the GS, as it results in the proper wave growth and phase propagation of the stream. However, as we have seen in case 2, the forecasts may lag the real ocean in a particular event, which may be taken care of by assimilating data during week 1 of the evolution. Also, it is worth noting that the MSFM scheme does not incorporate the change of temperature and salinity signature along the axis of the stream, and neither does it have a warm pool at the core of the stream. So, given the advantages and disadvantages of both OTIS and MSFM, it is our suggestion to incorporate the two important missing elements in the MSFM methodology, namely, (a) the longitudinal dependence of *T–S* relationship in the water-mass model and (b) provision of a warm pool at the core of the GS.

5. Conclusions

This paper concludes the three-part study of the circulation and dynamics of the western North Atlantic. The importance of multiscale feature models in representing the initial state of the GSMR region is shown via dynamical simulations. The Harvard PE model was calibrated and statistically validated earlier in Part II of this study. We used the calibrated model for generating 2- and 3-week-long simulations for three real synoptic case studies that have been studied by other investigators as well. The SBS simulations are compared with OTIS and NOSBS simulations for the same period using the same dynamical model.

By subjectively measuring the event formation and realistic behavior of the simulations, we find that the SBS simulations are better than either the OTIS or the NOSBS simulations for 2–3-week periods. There is little difference between SBS and NOSBS except for ring–stream interaction regions in the first week of simulations. From the objective measure of the offset statistic, in two out of three cases, SBS simulations did better (20%–37% better than persistence) than the other two in the first week; OTIS did better than the other two in

the other case. In fact, there are features in the OTIS fields, like the longitudinally varying water-mass structure and the warm pool in the core of the GS, that could be incorporated in the MSFM-based initializations. Surprisingly, the NOSBS simulation did better than the rest in case 3 for the second week, which we attributed to a correct ring–stream interaction captured by this simulation during the second week. During the second week, the SBS simulations are more realistic and does 15%–38% better than persistence in the other two cases.

Finally, it is proven from this series of studies that we can successfully predict (without assimilation) the evolution of the GS system for a period of 2 weeks with definitely better statistics than persistence and, in some cases, this prediction is still good for the third week using the multiscale feature model initializations. Note that the inclusion of surface forcing, such as wind stress, thermal, and buoyancy fluxes, could further improve the forecast skill of the simulations beyond the 2–3-week period achieved by the current methodology. We attribute the success of the MSFM-based forecasts to two factors: 1) kinematic synthesis of realistic feature models in the background circulation of the region in the initial state and 2) the calibration and validation of the primitive equation dynamical model to the synoptic dynamics of the GSMR region. It will be interesting to extend this methodology to other oceanic regions, to other scales, and to the climate modeling efforts.

Acknowledgments. This study was supported by the Office of Naval Research (N00014-93-1-0577) through a contract to Harvard University. A. Gangopadhyay had completed the writing while working at JPL on a NASA project (530-21000-0-3237). The final figures were set by JPL Graphics for the Modeling Project (944-47172-0-3237). Dr. Aaron Lai kindly provided the OTIS datasets. Hindcast simulations were carried out at the large-scale supercomputer center at the Stennis Space Center and at the Pittsburg Supercomputer Center. We would also like to thank Dr. Carlos Lozano, Ms. Marsha Cormier, Mr. Wayne G. Leslie, and other members of the Harvard University Oceanography group for their support of this work at numerous instances.

REFERENCES

Bryan, K., and M. D. Cox, 1967: A numerical investigation of the oceanic general circulation. *Tellus,* **19,** 54–80.

Clancy, R. M., 1987: Real-time applied oceanography at the Navy's global center. *Mar. Technol. Soc. J.,* **21,** 33–46.

——, P. A. Phoebus, K. D. Pollack, and J. Cummings, 1990: Operational global scale ocean thermal analysis system. *J. Atmos. Oceanic Technol.,* **7,** 233–254.

Cornillon, P., and D. R. Watts, 1987: Satellite thermal infrared and inverted echo sounder determinations of the Gulf Stream northern edge. *J. Atmos. Oceanic Technol.,* **4,** 712–723.

Cummings, J. A., and M. J. Ignazewski, 1991: The Fleet Numerical Oceanography Center regional ocean analysis system. *Proc. Mar. Technol. Soc.,* New Orleans, LA, Marine Technological Society, 1123–1129.

Ezer, T., and G. L. Mellor, 1994: Continuous assimilation of GEOSAT altimeter data into a three-dimensional primitive equation Gulf Stream model. *J. Phys. Oceanogr.*, **24,** 832–847.

——, D. S. Ko, and G. L. Mellor, 1992: Modeling and forecasting the Gulf Stream. Oceanic and Atmospheric Nowcasting and Forecasting, *Mar. Technol. Soc. J.,* **26** (2), 5–14.

Fox, D. N., M. R. Carnes, and J. L. Mitchell, 1992: Characterizing major frontal systems: A nowcast/forecast system for the northwest Atlantic. *Oceanography,* **5,** 49–54.

——, ——, and ——, 1993: Circulation model experiments of the Gulf Stream using satellite derived fields. Naval Research Laboratory Formal Rep. NRL/FR/7323-92-9412, Stennis Space Center, MS, 45 pp. [Available from NRL-Stennis, Stennis Space Center, MS 39529.]

Gangopadhyay, A., A. R. Robinson, and H. G. Arango, 1997: Circulation and dynamics of the western North Atlantic. Part I: Multiscale feature models. *J. Atmos. Oceanic Techol.,* **14,** 1314–1332.

Glenn, S. M., and A. R. Robinson, 1994: Validation of an operational Gulf Stream forecasting model. *Qualitative Skill Assessment for Coastal Models,* AGU Estuarine/Coastal Series, Vol. 47, Amer. Geophys. Union, 469–499.

Hurlburt, H. E., 1986: Dynamic transfer of simulated altimeter data into subsurface information by a numerical ocean model. *J. Geophys. Res.,* **91,** 2372–2400.

——, D. N. Fox, and E. J. Metzger, 1990: Statistical inference of weakly correlated subthermocline fields from satellite altimeter data. *J. Geophys. Res.,* **95,** 11 375–11 409.

Lai, C. A., W. Qian, and S. M. Glenn, 1994: Data assimilation and model evaluation experiment datasets. *Bull. Amer. Meteor. Soc.,* **75,** 793–810.

Mellor, G. L., and T. Ezer, 1991: A Gulf Stream model and an altimetry assimilation scheme. *J. Geophys. Res.,* **96,** 8779–8794.

Robinson, A. R., 1992: Shipboard prediction with a regional forecast model. *Oceanogr. Soc. Mag.,* **5** (1), 42–48.

——, and A. Gangopadhyay, 1997: Circulation and dynamics of the western North Atlantic. Part II: Dynamics of meanders and rings. *J. Atmos. Oceanic Techol.,* **14,** 1333–1351.

——, M. A. Spall, and N. Pinardi, 1988: Gulf Stream simulations and the dynamics of ring and meander processes. *J. Phys. Oceanogr.,* **18,** 1811–1853.

——, S. M. Glenn, M. A. Spall, L. J. Walstad, G. M. Gardner, and W. G. Leslie, 1989: Forecasting Gulf Stream meanders and rings. *EOS, Oceanogr. Rep.,* **70** (45), 1464–1473.

Spall, M. A., and A. R. Robinson, 1989: A new open ocean, hybrid coordinate primitive equation model. *Math. Comput. Simulation,* **31,** 241–269.

——, and ——, 1990: Regional primitive equation studies of the Gulf Stream meander and ring formation region. *J. Phys. Oceanogr.,* **20,** 985–1016.

Thompson, J. D., and W. J. Schmitz Jr., 1989: A limited-area model of the Gulf Stream: Design, initial experiments, and model-data intercomparisons. *J. Phys. Oceanogr.,* **19,** 792–814.

Willems, R. C., and Coauthors, 1994: Experiment evaluates ocean models and data assimilation in the Gulf Stream. *Eos, Trans. Amer. Geophys. Union,* **75,** 385–394.